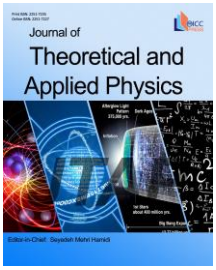

J. Theor. Appl. Phys 2026; 20(1): 19-32

Journal of Theoretical and Applied Physics (JTAP)

https://doi.org/10.57647/jtap.2026.2001.03

Research Article

Ion-Acoustic Wave Structures in a Collisionless Magnetised Plasma Considering (r, q)-Distributed Electrons and k-Distributed Positrons

Jintu Ozah[1*], P. N. Deka[2]

[1]*Department of Mathematics, Sibsagar University, Sivasagar-785665, Assam, India*
[2]*Department of Mathematics, Dibrugarh University, Dibrugarh-786004, Assam, India*

***Corresponding author:** jintuozah@gmail.com

Article History:

Received:
27 July 2025

Revised:
22 August 2025

Accepted:
25 October 2025

Published Online:
06 December 2025

Published in Issue:
28 February 2026

Abstract

This study addresses the properties of nonlinear ion-acoustic solitary waves (IASWs) within a magnetised plasma composed of ions, inertialess electrons, and positrons with a density gradient where electron and positron particles follow distinct non-Maxwellian energy distributions. To model this system, we derive a governing nonlinear evolution equation, known as the Zakharov-Kuznetsov (ZK) equation, using a standard reductive perturbation method (RPM). This equation is then analysed as a dynamical system to study the resulting solitary wave (SW) structures qualitatively. Through extensive numerical analysis, we investigate how physical parameters such as temperature and density ratios, the degree of non-thermality, the soliton velocity, the direction cosines, and the strength of the magnetic field affect the wave profile. A key finding is that, in contrast to the other non-thermal distributions, the amplitude of the solitary waves (SWs) is highest when the electron distribution approaches the standard Maxwellian case.

Keywords: magnetised plasma, κ -distribution, (r, q)-distribution, ion-acoustic waves, periodic waves, reductive perturbation method, ZK equation

Cite this article: Jintu O., Deka, P. N., (2026). Ion-acoustic wave structures in a collisionless magnetised plasma considering (r, q)-distributed electrons and k-distributed positrons. *J. Theor. Appl. Phys.,* 20(1), 19-32. https://doi.org/10.57647/jtap.2026.2001.03

1. Introduction

Electrostatic IASWs are the most widely investigated modes in both theoretical and experimental plasma physics research [1-6]. Solitons, a specific type of SW, represent nonlinear disturbances within a medium that exhibit the remarkable property of retaining their shape after collisions. The experimental observation of ion-acoustic solitons (IASs) was initially achieved by Ikezi [7] in a laboratory setting, and subsequently, further experimental studies were carried out on double plasma devices. The significance of solitons has been recognised across diverse fields over the past century, including solid-state physics [8], fluid dynamics [9], medicine [10], astrophysics [11], and space physics [12]. Their importance in plasma physics remains particularly relevant due to their influence on energy transport phenomena. IASs have been investigated in both unmagnetised and magnetised plasmas using either the RPM or the fully nonlinear pseudopotential approach [7, 13, 14]. Electron-positron-ion (e-p-i) plasmas, remarkably, constituted a significant portion of the early universe and are currently observed in diverse astrophysical environments, including pulsar magnetospheres [15, 16], active galactic nuclei [17], solar

atmospheres [18], and accretion disks [19]. A considerable body of research over the past few decades has explored IASWs within e-p-i plasmas, encompassing both thermal and non-thermal velocity distributions for the electrons and positrons [20-27]. El-Labany et al. [28] observed the nonlinear solitary and shock waves in a rotating weakly relativistic plasma containing electron, positron and stationary positive ion particles. Chatterjee and Ghosh [29] employed the extended Poincaré-Lighthill-Kuo (PLK) method to investigate head-on collisions of IASWs in an e-p-i plasma. Their study considered a plasma composition of inertial ions alongside superthermal electrons and positrons. Saini et al. [30] investigated the features of large-amplitude SWs and double layers in e-p-i plasmas containing negatively charged dust grains. Utilising the Sagdeev pseudopotential method, they derived the energy balance equation and identified the critical Mach number necessary for SW existence. Singh et al. [31] employed fluid simulations to study the development of IASWs in the context of pulsar winds. Their model considered a weakly relativistic, unmagnetised, and collisionless plasma composed of inertial relativistic ions alongside superthermal electrons and positrons. Recently, the dynamics of soliton and conoidal solutions of the damped Kawahara equation have been studied by El-Awady et al. [32] in an e-p-i plasma considering Landau quantisation effects. The characteristics of nonlinear wave structures are demonstrably dependent on the shape of particle distribution functions, which are essential in determining wave dynamics [33, 34]. Many satellite observations have claimed that the particles in the space environment often deviate from the Maxwellian equilibrium due to the higher energy tails and exist shoulders or flat tops in the lower energy region of the distribution functions [35, 36]. To explain the observed density depletion structures by Freja and Viking satellites, Cairns et al. [37] incorporated a non-thermal electron distribution function into their plasma model. These structures deviate from predictions based on the Maxwellian distribution. However, particle distributions with a significant abundance of superthermal particles are often better characterised by the κ -distribution function compared to the Maxwellian distribution. κ -distributions with a kappa index (κ) ranging from 2 to 6 have been shown to provide a good fit to observations and satellite data in various space plasma environments, including the solar wind [38], the terrestrial magnetosphere [39], the terrestrial plasma sheet [40], and the magnetosheath [41], and so on. However, observations in some space plasma regions reveal electron distributions that deviate from kappa and Cairns distributions, exhibiting modified tails and flat tops. In an effort to more comprehensively account for observed phenomena in space plasmas, Qureshi et al. [42] proposed a novel non-Maxwellian distribution function over a decade ago. This distribution incorporates two spectral indices, r and q, in contrast to the single index employed in the κ -distribution function. The (r, q)-distribution is a powerful tool used in plasma physics to describe the velocity distribution of electrons. It offers a significant advantage over other distribution functions due to its versatility. By adjusting the two parameters, r and q, the (r, q)-distribution can effectively mimic the behaviour of a wide range of other distributions [41]. Considering the (r, q)-distributed electron species, Sehar et al. [43] studied the electron acoustic instability in a four-component space plasma. An observation has been made on electron acoustic structure by Albalawi et al. [44] in a non-Maxwellian plasma having (r, q)-distributed two-temperature electrons. Shumaila [45] et al. carried out an observation of the characteristics of electrostatic waves on Saturn's magnetosphere, where the electron particles follow (r, q)-distribution.

The RPM is mostly effective for the study of the dynamics of IASWs in a nonlinear complex system. This method reduces the complex nonlinear set of governing equations into a simplified form of partial differential equation, such as the Korteweg-de Vries (K-dV) type equation, the ZK equation, etc., that effectively balances the nonlinearity and dispersion of the nonlinear regimes. As compared to the other analytical methods, the RPM is simpler and easier to apply in a multicomponent plasma system, where the exact solutions are frequently difficult to find. Moreover, RPM is widely used and well-established in plasma physics for analysing small but finite amplitude nonlinear waves, making it an appropriate and reliable method for the present investigation. Habib et al. [46] theoretically investigated dust acoustic solitary waves (DASWs) in an electron-depleted, nonthermal magnetised plasma, deriving the nonlinear ZK equation using the RPM. In another theoretical work, Atteya et al. [47] studied the nonlinear periodic and superperiodic waves in a degenerate multi-ion plasma. The modified ZK equation was derived for the ion-acoustic waves (IAWs) using the RPM.

Bifurcation theory has emerged as a prominent and powerful tool in recent years for investigating the dynamical behaviour of plasma systems. The trajectories traced within a dynamical system's phase portrait map onto distinct nonlinear wave solutions of the plasma model. Therefore, bifurcation analysis of the Hamiltonian system's phase portrait has become a widely employed technique to unveil the physical behaviour of travelling nonlinear acoustic waves in plasmas. In this vein, Selim et al. [48] utilised bifurcation analysis to explore the properties of nonlinear ion-acoustic travelling waves through a magnetised plasma composed of multiple components, including electrons with superthermal energy distributions. Kolay et al. [49] employed bifurcation analysis to

investigate nonlinear ion-acoustic wave (IAW) structures due to Martian ionospheric loss, where electrons follow a generalised (r, q)-distribution. Pradhan et al. [50] have applied the bifurcation analysis to explore the characteristics of IASWs in multi-species cometary plasma with κ -distributed electrons. This plasma comprised warm fluid ions, ultrarelativistic degenerate electrons and positrons, alongside immobile heavy negative ions. Ali et al. [51] studied the ion-acoustic solitary and periodic structure along with the dynamical system in a magnetised two-ion component ($O^+ - H^+ - e$) dusty plasma with (r, q)-distributed electrons. It was found that the propagation behaviour of nonlinear ion-acoustic solitary structures exhibits distinct characteristics for fast and slow modes due to their inherently different physical underpinnings. Atteya et al. [52] recently investigated the bifurcation of nonlinear electron-acoustic waves (EAWs) propagating in a collisionless, unmagnetised plasma where electrons are modelled by a κ -distribution. Despite the growing interest in e-p-i plasmas with κ -distributed electrons and positrons, a critical knowledge gap remains regarding ion dynamics under the influence of these non-Maxwellian species. While the recent investigation by El-Monier et al. [53] provides valuable insight into the bifurcation of IAWs in a plasma comprised of kappa-distributed hot solar and cold cometary electrons, their analysis does not extend to the broader influence of the electron distribution function's specific parameters on the fundamental dynamics of these waves, which constitutes the principal objective of the present study. A comprehensive investigation incorporating the full distribution profile is paramount to elucidating the complete interplay within this complex plasma system. Therefore, in this work, we investigate IASWs propagating with the bifurcation analysis within an e-p-i plasma characterised by electrons with (r, q)-distribution and positrons with k-distribution.

2. Governing equations

For this study, a three-dimensional plasma system is considered with non-Maxwellian electron and positron particles having a density gradient. A background magnetic field $B = B\hat{e}_x$ is considered along the direction of the x -axis. The normalised form of the governing equations that represent the plasma system is considered as follows:

$$\frac{\partial n_i}{\partial t} + \nabla(n_i u_i) = 0 \tag{1}$$

$$\frac{\partial u_i}{\partial t} + (u_i.\nabla).u_i + \frac{3\sigma}{n_i}\nabla n_i = -\nabla\phi + u_i \times \Omega_{Bi} \tag{2}$$

$$\nabla^2\phi - n_e + n_i + n_p = 0 \tag{3}$$

The normalised form of the (r, q)-distribution function for the electron population is defined as [54, 55]

$$n_e = \left(1 + A_{rq}\phi + B_{rq}\phi^2\right) \tag{4}$$

where

$$A_{rq} = \frac{(q-1)^{-\frac{1}{(1+r)}}}{2C}\frac{\Gamma\left(\frac{1}{2(1+r)}\right)\Gamma\left(q-\frac{1}{2(1+r)}\right)}{\Gamma\left(\frac{3}{2(1+r)}\right)\Gamma\left(q-\frac{3}{2(1+r)}\right)},$$

$$B_{rq} = \frac{3(q-1)^{-\frac{2}{(1+r)}}}{8C^2}\frac{\Gamma\left(1-\frac{1}{2(1+r)}\right)\Gamma\left(q+\frac{1}{2(1+r)}\right)}{\Gamma\left(1+\frac{3}{2(1+r)}\right)\Gamma\left(q-\frac{3}{2(1+r)}\right)}$$

and

$$C = \frac{3(q-1)^{-\frac{1}{(1+r)}}\Gamma\left(q-\frac{3}{2+2r}\right)\Gamma\left(\frac{3}{2+2r}\right)}{2\Gamma\left(q-\frac{5}{2+2r}\right)\Gamma\left(\frac{5}{2+2r}\right)}$$

In the above, r and q are two spectral indices that determine the shoulders and tail of the distribution function, satisfying the conditions $q > 1$ and $q(r+1) > \frac{5}{2}$. A primary validation of our model's integrity is its correct reduction to well-known distribution functions in specific limits. At the limit $r = 0$ and $q \to \infty$, the distribution function (4) is transferred to the Maxwellian distribution, and the coefficients A_{rq} and B_{rq} have the form $A_{rq} = 1$ and $B_{rq} = \frac{1}{2}$. Also, when $r = 0$ and $q \to (\kappa + 1)$, the distribution function (4) reduces to the κ -distribution with the coefficients $A_{rq} = \frac{\kappa_e - \frac{1}{2}}{\kappa_e - \frac{3}{2}}$ and $B_{rq} = \frac{\left(\kappa_e - \frac{1}{2}\right)\left(\kappa_e + \frac{1}{2}\right)}{2\left(\kappa_e - \frac{3}{2}\right)^2}$.
This is a standard and powerful technique, also used in Refs. [56-58].
The positron number density is given by the κ -distribution [59] as follows:

$$n_p = p\left(1 + \frac{\delta\phi}{\left(\kappa_p - \frac{3}{2}\right)}\right)^{-\kappa_p + \frac{1}{2}} \tag{5}$$

$$n_p = p(1 - \delta A_\kappa\phi + \delta^2 B_\kappa\phi^2)$$

where $\delta = \frac{T_e}{T_p}$, $\sigma = \frac{T_i}{T_e}$, $p = \frac{n_{p0}}{n_{e0}}$, $A_\kappa = \frac{\left(\kappa_p - \frac{1}{2}\right)}{\left(\kappa_p - \frac{3}{2}\right)}$, $B_\kappa = \frac{\left(\kappa_p - \frac{1}{2}\right)\left(\kappa_p + \frac{1}{2}\right)}{2\left(\kappa_p - \frac{3}{2}\right)^2}$.
In the limit, when $\kappa_p \to \infty$, the above κ -distribution function reduces to the Maxwellian distribution form with the coefficients $A_\kappa = 1$ and $B_\kappa = \frac{1}{2}$.
In the above equations, n_e, n_p, and n_i are number densities of electrons, positrons, and ions, respectively, normalised by the unperturbed electron density. Ω_{Bi} is the ion-cyclotron frequency. Ion fluid velocity $\vec{u}_i$ is normalised by

10.57647/jtap.2026.2001.03

$u_s = \left(\frac{k_B T_e}{m_i}\right)^{\frac{1}{2}}$, where k_B is the Boltzmann constant and T_e is the temperature of electrons. The electrostatic potential ϕ is normalised by $\frac{k_B T_e}{e}$. The space coordinates (x, y, z) and time t are normalised by the electron Debye length $\lambda_D = \left(\frac{k_B T_e}{4\pi e^2 n_0}\right)^{\frac{1}{2}}$ and the inverse of plasma frequency $\omega_p^{-1} = \left(\frac{m_1}{4\pi n_0 e^2}\right)^{\frac{1}{2}}$, respectively.

3. Nonlinear analysis

To obtain the nonlinear ZK equation, we have applied the RPM. To study the nonlinear wave formation in our plasma system, we have introduced the following appropriate stretched coordinates [60-63]

$$\xi = \varepsilon^{\frac{1}{2}}(x - \lambda_0 t),\ \eta = \varepsilon^{\frac{1}{2}} y,\ \zeta = \varepsilon^{\frac{1}{2}} z,\ \tau = \varepsilon^{\frac{3}{2}} t. \tag{6}$$

Here, ε is a small quantity measuring the strength of nonlinearity. λ_0 is the phase velocity of IASWs. Stretching the coordinates helps us see in detail what happens on different scales of distance or time. Different stretching is required for different physical problems because of the different small domains over which interesting physics may take place.

The physical quantities are expanded in the power series expansion of ε in the following way

$$\begin{aligned} n_i &= 1 + \varepsilon^1 n^1 + \varepsilon^2 n^2 + \varepsilon^3 n^3 + \ldots \\ u &= \varepsilon^1 u^1 + \varepsilon^2 u^2 + \varepsilon^3 u^3 + \ldots \\ v &= \varepsilon^{\frac{3}{2}} v^1 + \varepsilon^2 v^2 + \varepsilon^{\frac{5}{2}} v^3 + \ldots \\ w &= \varepsilon^{\frac{3}{2}} w^1 + \varepsilon^2 w^2 + \varepsilon^{\frac{5}{2}} w^3 + \ldots \\ \phi &= \varepsilon^1 \phi^1 + \varepsilon^2 \phi^2 + \varepsilon^3 \phi^3 + \ldots \end{aligned} \tag{7}$$

After applying the stretching coordinates (6) in the governing Eqs. (1) - (3), one can obtain the following equations:

$$-\lambda_0 \varepsilon^{\frac{1}{2}} \frac{\partial n_i}{\partial \xi} + \varepsilon^{\frac{3}{2}} \frac{\partial n_i}{\partial \tau} + \varepsilon^{\frac{1}{2}} \frac{\partial (n_i u)}{\partial \xi} + \varepsilon^{\frac{1}{2}} \frac{\partial (n_i v)}{\partial \eta} + \varepsilon^{\frac{1}{2}} \frac{\partial (n_i w)}{\partial \zeta} = 0 \tag{8}$$

$$-\lambda_0 \varepsilon^{\frac{1}{2}} \frac{\partial u}{\partial \xi} + \varepsilon^{\frac{3}{2}} \frac{\partial u}{\partial \tau} + u\varepsilon^{\frac{1}{2}} \frac{\partial u}{\partial \xi} + v\varepsilon^{\frac{1}{2}} \frac{\partial u}{\partial \eta} + w\varepsilon^{\frac{1}{2}} \frac{\partial u}{\partial \zeta} + \frac{3\sigma}{n_i} \varepsilon^{\frac{1}{2}} \frac{\partial n_i}{\partial \xi} = -\varepsilon^{\frac{1}{2}} \frac{\partial \phi}{\partial \xi} \tag{9}$$

$$-\lambda_0 \varepsilon^{\frac{1}{2}} \frac{\partial v}{\partial \xi} + \varepsilon^{\frac{3}{2}} \frac{\partial v}{\partial \tau} + u\varepsilon^{\frac{1}{2}} \frac{\partial v}{\partial \xi} + v\varepsilon^{\frac{1}{2}} \frac{\partial v}{\partial \eta} + w\varepsilon^{\frac{1}{2}} \frac{\partial v}{\partial \zeta} + \frac{3\sigma}{n_i} \varepsilon^{\frac{1}{2}} \frac{\partial n_i}{\partial \eta} = -\varepsilon^{\frac{1}{2}} \frac{\partial \phi}{\partial \eta} + w \times \Omega_{Bi} \tag{10}$$

$$-\lambda_0 \varepsilon^{\frac{1}{2}} \frac{\partial w}{\partial \xi} + \varepsilon^{\frac{3}{2}} \frac{\partial w}{\partial \tau} + u\varepsilon^{\frac{1}{2}} \frac{\partial w}{\partial \xi} + v\varepsilon^{\frac{1}{2}} \frac{\partial w}{\partial \eta} + w\varepsilon^{\frac{1}{2}} \frac{\partial w}{\partial \zeta} + \frac{3\sigma}{n_i} \varepsilon^{\frac{1}{2}} \frac{\partial n_i}{\partial \zeta} = -\varepsilon^{\frac{1}{2}} \frac{\partial \phi}{\partial \zeta} - v \times \Omega_{Bi} \tag{11}$$

$$\varepsilon \frac{\partial^2 \phi}{\partial \xi^2} + \varepsilon \frac{\partial^2 \phi}{\partial \eta^2} + \varepsilon \frac{\partial^2 \phi}{\partial \zeta^2} - n_e + n_i + n_p = 0 \tag{12}$$

Now, substituting the power series expansions from Eq. (7) into the above Eqs. (8) - (12), and collecting the terms of the lowest order in ε, we obtain the following set of equations:

$$\begin{aligned} n_i^1 &= \frac{u^1}{\lambda_0},\ u^1 = \frac{\phi^1 + 3\sigma n_i^1}{\lambda_0},\ v^1 = -\frac{1}{\Omega_{Bi}} \left(\frac{\partial \phi^1}{\partial \zeta} + 3\sigma \frac{\partial n_i^1}{\partial \zeta}\right) \\ w^1 &= \frac{1}{\Omega_{Bi}} \left(\frac{\partial \phi^1}{\partial \eta} + 3\sigma \frac{\partial n_i^1}{\partial \eta}\right),\ \phi^1 = \frac{n_i^1}{A_{rq} + p\delta A_k} \end{aligned} \tag{13}$$

By simultaneously solving the algebraic relations in Eq. (13), we eliminate n_i^1 and u^1 to obtain the following phase velocity for the IAWs

$$\lambda_0 = \sqrt{3\sigma + \frac{1}{A_{rq} + p\delta A_k}} \tag{14}$$

We proceed to the next orders of ε. The process is methodical but lengthy; we summarise the key equations obtained at $O\left(\varepsilon^{\frac{3}{2}}\right)$ and $O(\varepsilon^2)$ that relate the second-order perturbed quantities n_i^2, u^2, ϕ^2, etc., and the higher-order equations are obtained as

$$v^2 = \frac{\lambda_0}{\Omega_{Bi}} \frac{\partial w^1}{\partial \xi} \tag{15}$$

$$w^2 = -\frac{\lambda_0}{\Omega_{Bi}} \frac{\partial v^1}{\partial \xi} \tag{16}$$

$$\frac{\partial n_i^1}{\partial \tau} - \lambda_0 \frac{\partial n_i^2}{\partial \xi} + \frac{\partial u^2}{\partial \xi} + \frac{\partial v^2}{\partial \eta} + \frac{\partial w^2}{\partial \zeta} + \frac{\partial (n_i^1 u^1)}{\partial \xi} = 0 \tag{17}$$

$$\frac{\partial u^1}{\partial \tau} + u^1 \frac{\partial u^1}{\partial \xi} - \lambda_0 n_i^1 \frac{\partial u^1}{\partial \xi} - \lambda_0 \frac{\partial u^2}{\partial \xi} + 3\sigma \frac{\partial n_i^2}{\partial \xi} + n_i^1 \frac{\partial \phi^1}{\partial \xi} + \frac{\partial \phi^2}{\partial \xi} = 0 \tag{18}$$

$$\frac{\partial^2 \phi^1}{\partial \xi^2} + \frac{\partial^2 \phi^1}{\partial \eta^2} + \frac{\partial^2 \phi^1}{\partial \zeta^2} + n_i^2 - (A_{rq} + p\delta A_k)\phi^2 \tag{19}$$

$$-\frac{1}{2}(B_{rq}-pB_k\delta^2)(\phi^1)^2=0$$

Using the lowest-order equations obtained in Eq. (13) and the phase velocity relation (14) in Eqs. (15) - (19) and after eliminating higher-order quantities, we have obtained the ZK equation in the following form

$$\frac{\partial\phi^1}{\partial\tau}+\alpha\phi^1\frac{\partial\phi^1}{\partial\xi}+\beta\frac{\partial^3\phi^1}{\partial\xi^3}+\gamma\frac{\partial}{\partial\xi}\left(\frac{\partial^2\phi^1}{\partial\eta^2}+\frac{\partial^2\phi^1}{\partial\zeta^2}\right)=0 \quad (20)$$

where $\alpha=\frac{1}{2\lambda_0}+\frac{\lambda_0}{\lambda_0^2-3\sigma}-\frac{(\lambda_0^2-3\sigma)^2}{\lambda_0}(B_{rq}-pB_k\delta^2)$ is the nonlinear coefficient, and $\beta=\frac{(\lambda_0^2-3\sigma)^2}{2\lambda_0}$, and $\gamma=\frac{(\lambda_0^2-3\sigma)^2}{2\lambda_0}+\frac{\lambda_0^3}{2\Omega_{Bi}^2}$. For the qualitative phase plane analysis, the planar dynamical system corresponding to the ZK Eq. (20) is presented here. For this, we have considered a standard transformation $\chi=l_x\xi+l_y\eta+l_z\zeta-u\tau$, where l_x, l_y, and l_z are direction cosines. By setting $\phi^1(\xi,\eta,\zeta,\tau)=\psi(\chi)$, the above ZK Eq. (20) is reduced to the following ordinary differential equation

$$-u\frac{d\psi}{d\chi}+\frac{\alpha}{2}l_x\frac{d\psi^2}{d\chi}+l_x\left[\beta l_x^2+\gamma\left(l_y^2+l_z^2\right)\right]\frac{d^3\psi}{d\chi^3}=0 \quad (21)$$

After integrating with respect to χ, the following dynamical system of equations can be obtained as

$$\begin{cases}\frac{d\psi}{d\chi}=z,\\ \frac{dz}{d\chi}=\frac{u}{l_x\left[\beta l_x^2+\gamma\left(l_y^2+l_z^2\right)\right]}\psi-\frac{\alpha}{2\left[\beta l_x^2+\gamma\left(l_y^2+l_z^2\right)\right]}\psi^2.\end{cases} \quad (22)$$

The corresponding Hamiltonian function is

$$H=\frac{z^2}{2}+\frac{(\alpha l_x\psi-3u)\psi^2}{6l_x\left[\beta l_x^2+\gamma\left(l_y^2+l_z^2\right)\right]} \quad (23)$$

and the Sagdeev pseudopotential function of the system is given by

$$V(\psi)=\frac{(\alpha l_x\psi-3u)\psi^2}{6l_x\left[\beta l_x^2+\gamma\left(l_y^2+l_z^2\right)\right]} \quad (24)$$

The SW solution [64] corresponding to Eq. (20) is given as

$$\phi^1=\phi_m\,sech^2\left(\frac{\chi}{W}\right) \quad (25)$$

where $\phi_m=\frac{3u}{\alpha l_x}$ and $W=\left[\frac{4l_x\left(\beta l_x^2+\gamma\left(l_y^2+l_z^2\right)\right)}{u}\right]^{\frac{1}{2}}$.

4. Results and discussion

The ZK Eq. (20) is a familiar nonlinear equation used to study the formation of nonlinear waves in a magnetised plasma system. This equation has a solution defined in Eq. (25), which is dependent on the coefficients appearing in the ZK equation.

Here for a detailed study and to incorporate the nonlinear travelling solitary and periodic waves (PWs), we have transferred the ZK Eq. (20) into a planar dynamical system of Eqs. (22) and discussed the qualitative dynamics of the system elaborately.

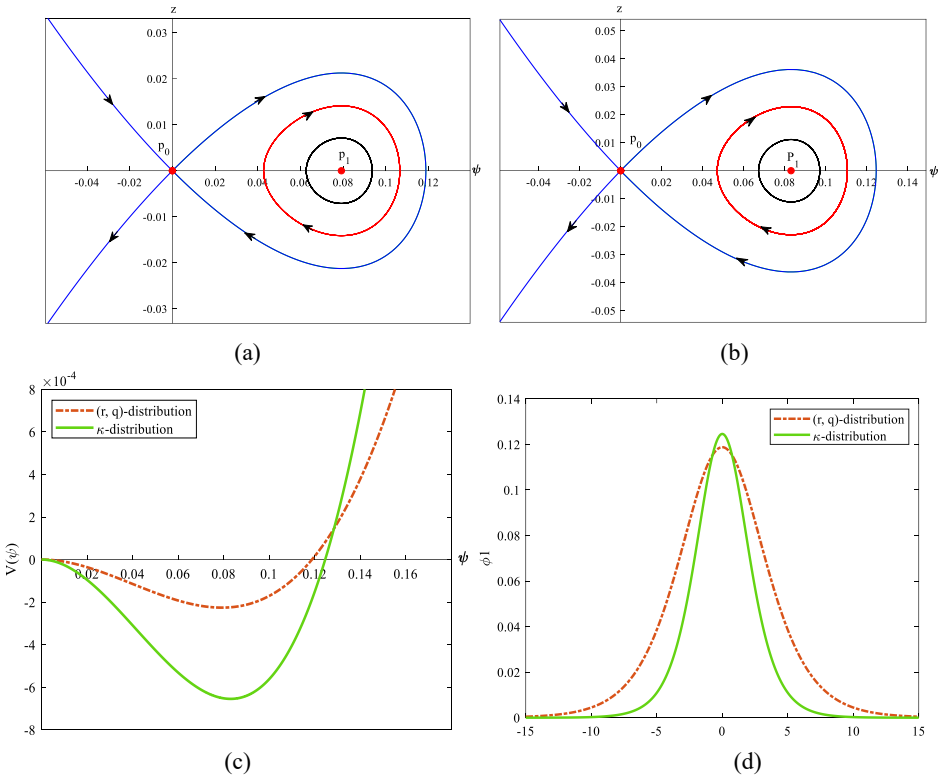

Figure 1. Phase space dynamics of the system (22), (a) for (r, q)-distribution, (b) for κ -distribution, (c) pseudopotential curves $V(\psi)$ against ψ, (d) corresponding SW structure, with different values of parameters $\kappa_e=\kappa_p=2$, $u=0.1$, $l_x=0.8$, $r=3$, $q=2$, $p=0.4$, $\delta=1$, $\sigma=0.05$, and $\Omega_{Bi}=0.5$

The numerical values of the parameters used for the study are $\kappa_p = 2, u = 0.1, l_x = 0.8, r = 3, q = 2, p = 0.4, \delta = 1, \sigma = 0.05$, and $\Omega_{Bi} = 0.5$ [65]. The phase portrait profile of the dynamical system (22) and the pseudopotential curves (24) are depicted in Figures. 1(a)-(c) for two different cases of (r, q)-distribution and κ -distribution. Figure 1(a) illustrates the phase plane for the (r, q)-distributed function. A similar kind of graphical representation of a phase plot diagram for the limiting case of κ -distribution is shown in Figure 1(b). From the phase portrait diagrams, it is clear that the dynamical system (22) has two equilibrium points, $P_0(0,0)$ and $P_1\left(\frac{2u}{\alpha l_x}, 0\right)$, where P_0 is the saddle point and P_1 is the centre point, respectively. Depending on the sign of α, whether it is positive or negative, the centre point P_1 lies in either the positive or negative direction of the ψ -axis. In this case, the sign of the nonlinear coefficient α is positive; hence, the equilibrium point P_1 appears in the positive direction of the ψ -axis and results in the compressive SWs. In the phase diagrams, the periodic trajectories have confirmed the presence of PWs in the plasma system, whereas the homoclinic trajectories signify the existence of SWs. The Sagdeev pseudopotential curve for Eq. (24) is depicted in Figure 1(c). The dot-dash curve corresponds to the IASWs for (r, q)-distributed electrons, and the solid curve corresponds to the IASWs for κ -distribution electrons. The SW profiles corresponding to the homoclinic trajectories obtained in Figures. 1(a) and 1(b) are presented in Figure 1(d). Figure 2(a) illustrates the nonlinear PWs for the black-coloured periodic trajectories obtained in Figures 1(a) and 1(b). Similarly, PWs for the red-coloured periodic trajectories found in Figures 1(a) and 1(b) have been plotted in Figure 2(b).

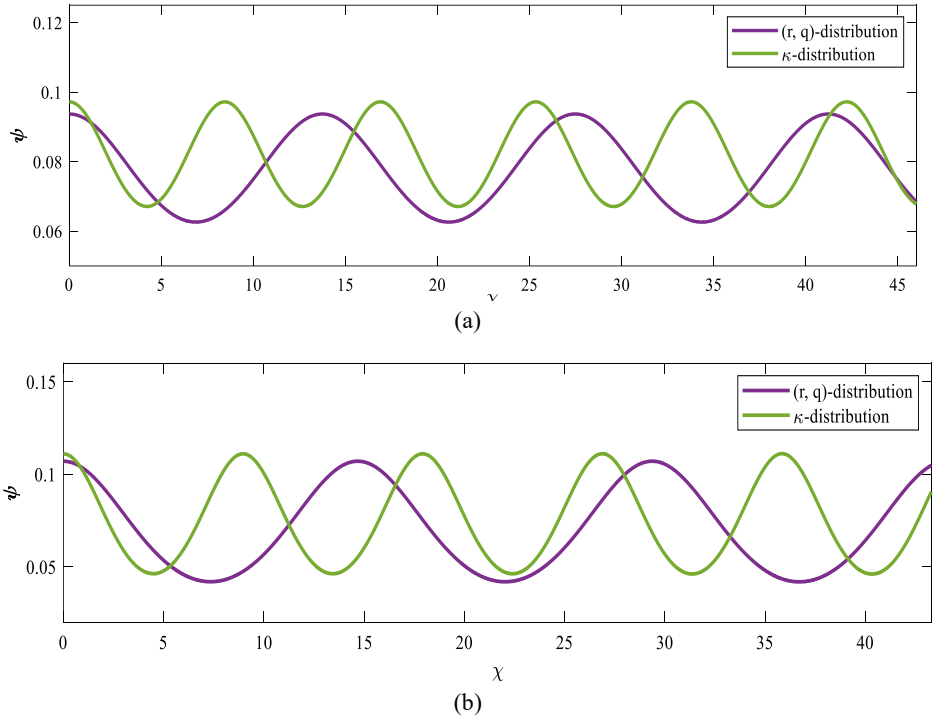

Figure 2. PW structures for the periodic trajectories, with different values of the parameters $\kappa_e = \kappa_p = 2, u = 0.1, l_x = 0.8, r = 3, q = 2, p = 0.4, \delta = 1, \sigma = 0.05$, and $\Omega_{Bi} = 0.5$

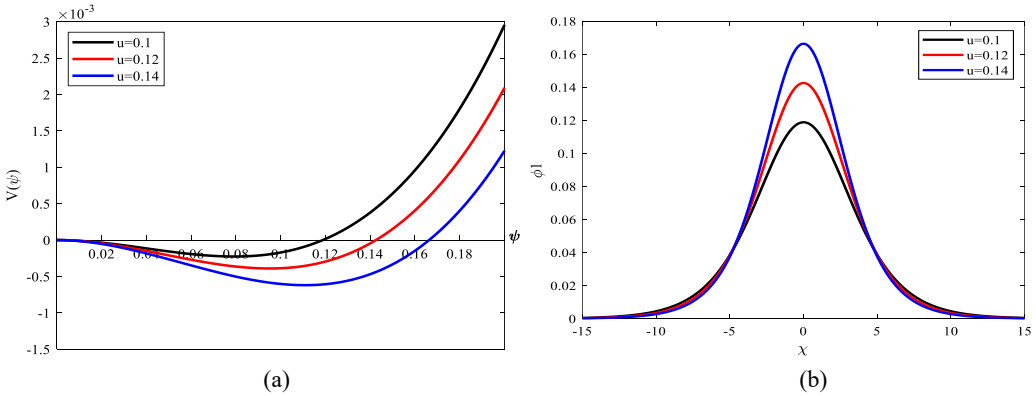

Figure 3. Variation of (a) pseudopotential function $V(\psi)$ and (b) structure of IASWs, for different values of wave velocity (u), with the parameters $\kappa_p = 2, l_x = 0.8, r = 3, q = 2, p = 0.4, \delta = 1, \sigma = 0.05$, and $\Omega_{Bi} = 0.5$

10.57647/jtap.2026.2001.03

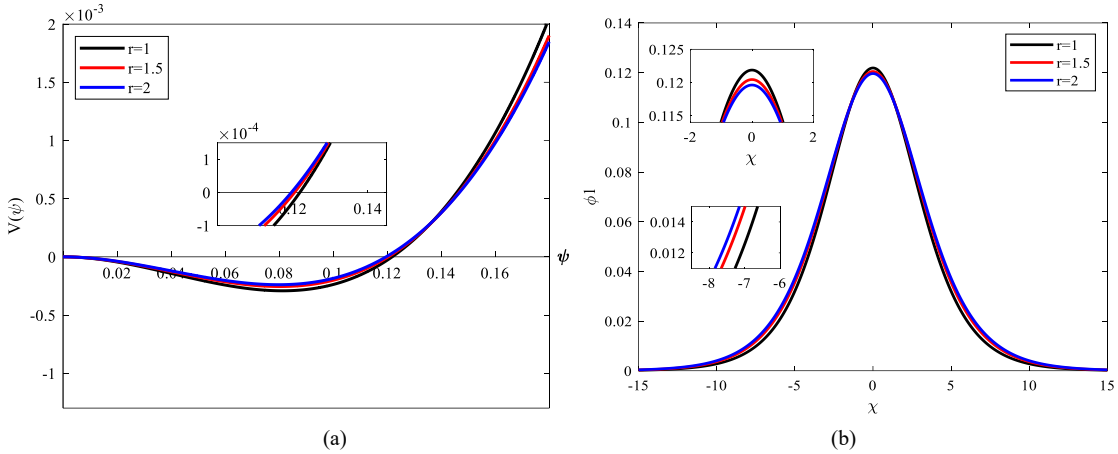

(a) (b)

Figure 4. Variation of (a) pseudopotential function $V(\psi)$ and (b) structure of IASWs, for different values of spectral index parameter (r), with the parameters $\kappa_p = 2$, $u = 0.1$, $l_x = 0.8$, $q = 2$, $p = 0.4$, $\delta = 1$, $\sigma = 0.05$, and $\Omega_{Bi} = 0.5$

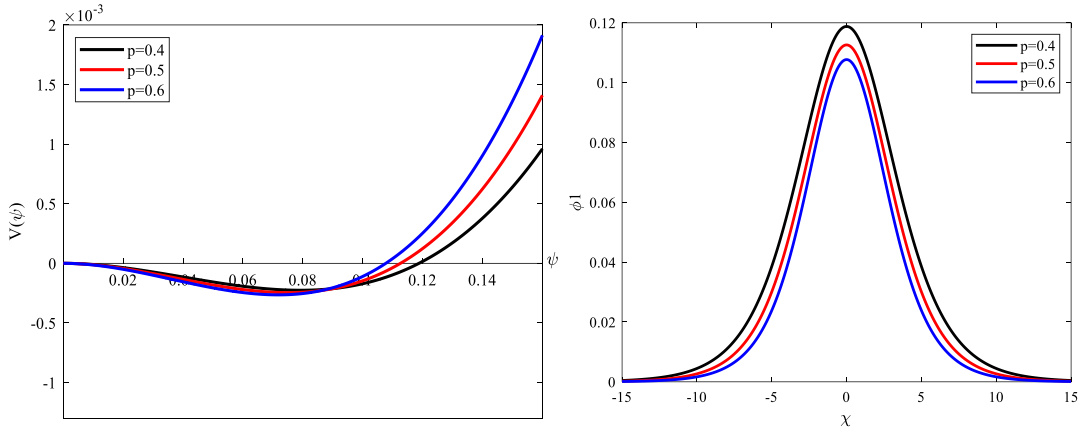

(a) (b

Figure 5. Variation of (a) pseudopotential function $V(\psi)$ and (b) structure of IASWs, for different values of positron-to-electron density ratio (p), with the parameters $\kappa_p = 2$, $u = 0.1$, $l_x = 0.8$, $q = 2$, $\delta = 1$, $\sigma = 0.05$, $r = 3$, and $\Omega_{Bi} = 0.5$

Now, the nonlinear characteristics of IASWs and PWs are studied through the numerical analysis with the variations of different plasma parameters, such as positron-to-electron density ratio (p), ion-electron temperature ratio (σ), spectral indices $(r,q,$ and $\kappa_p)$, wave velocity (u), direction cosines $(l_x l_y,$ and $l_z)$, and the background magnetic field (Ω_{Bi}), respectively. First, we have plotted the profiles of potential function $V(\psi)$ and IASWs in Figures 3(a) and (b) for three distinct values of wave velocity (u).

It can be seen that enhancing the wave velocity raises the amplitude of IASWs. On the contrary, the width of the SWs is seen to decrease along with the increasing values of u. The variation of the potential curve and the IASWs are shown in Figures 4(a) and (b) for three different values of the spectral index parameter r.

The graphical analysis of data reveals that the amplitude of the SWs shows a negative correlation, and the width shows a positive correlation with the spectral index r, i.e., as the values of r increase, the SW amplitude decreases while its width is raised.

Figure 5 shows the impact of the positron-to-electron density ratio (p) on the potential function $V(\psi)$ and the characteristics of SWs. The profile of SWs exhibits that the amplitude is decreased with the increasing values of density ratio p. Also, along with the increasing values of p, the width is shown to have the same behaviour. Thus, the positron-to-electron density ratio negatively impacts the formation of IASWs. Figures 6(a) and (b) depict the variation of potential function $V(\psi)$ and the profile of IASWs for three distinct values of ion-to-electron temperature ratio (σ). The graphical results show that initially, the amplitude of IASWs is growing as the temperature ratio σ is increased. But after particular values of σ, the amplitude is seen to be decreasing. On the other hand, the width of the SWs remains increased as σ increases. The graphical representation shown in Figure 7 illustrates the correlation between the influence of the background magnetic field effect (Ω_{Bi}) on the potential curve $V(\psi)$ and the SW profile. The results clearly show that the background magnetic field reduces the width of the SWs

10.57647/jtap.2026.2001.03

without having any visible change in the amplitude. To fully understand the characteristics of nonlinear PWs, we have illustrated some graphical representations of PWs in Figures 8 and 9 under the influence of several physical parameters such as l_x, κ_p, σ, and Ω_{Bi}. Figure 8(a) depicts the ion-acoustic periodic wave (IAPW) profile as a function of space coordinate χ for three distinct values of l_x. From this figure, it is observed that the IAPW gets more height and more expansive as the values of l_x are increased. In Figure 8(b), the PW profile varies for three distinct values of the spectral index parameter κ_p, showing that the amplitude and the width of the periodic wave (PW) increase with an increasing value of κ_p. One can see from Figure 9(a) that the IAPW becomes more expanded as the parameter σ is augmented, while the amplitude does not have any visible change.

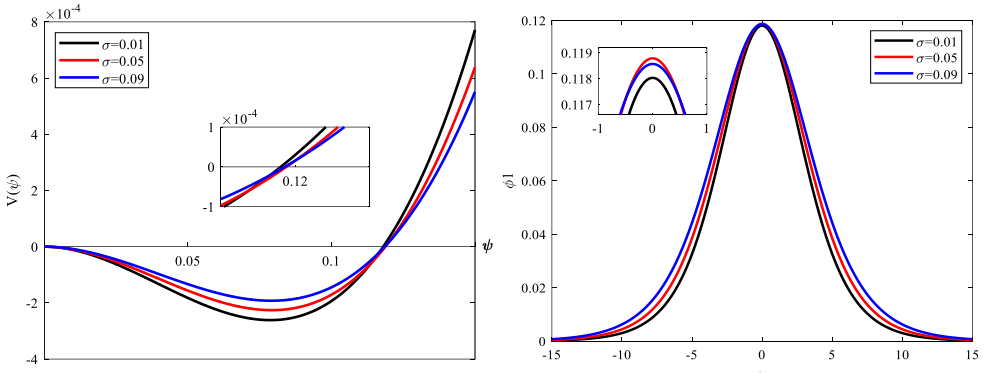

(a) (b)

Figure 6. Variation of (a) pseudopotential function $V(\psi)$ and (b) structure of IASWs for different values of ion-to-electron temperature ratio (σ), with the parameters $\kappa_p = 2$, $u = 0.1$, $l_x = 0.8$, $q = 2$, $\delta = 1$, $p = 0.4$, $r = 3$, and $\Omega_{Bi} = 0.5$

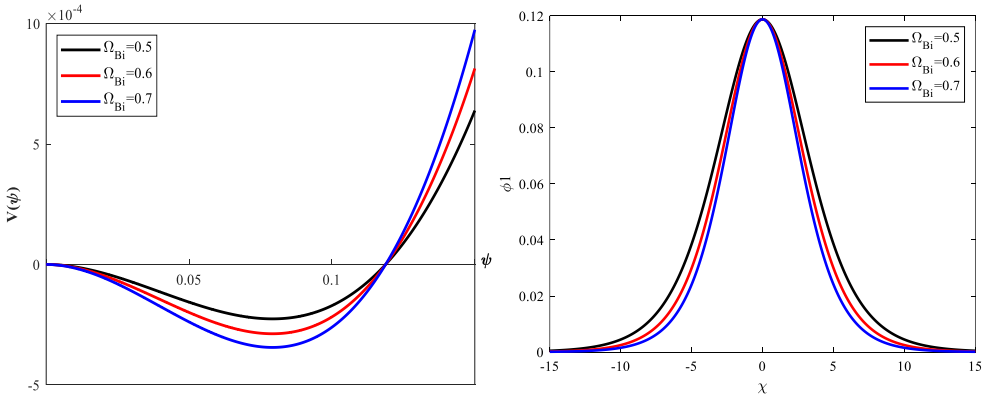

(a) (b)

Figure 7. Variation of (a) pseudopotential function $V(\psi)$ and (b) structure of IASWs, for different values of magnetic field effect (Ω_{Bi}), with the parameters $\kappa_p = 2$, $u = 0.1$, $l_x = 0.8$, $q = 2$, $\delta = 1$, $p = 0.4$, $r = 3$, and $\sigma = 0.05$

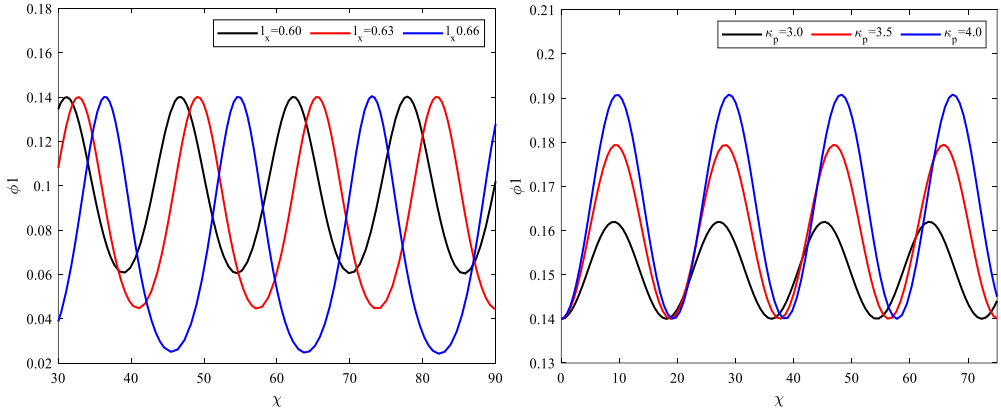

(a) (b)

Figure 8. The evolution of the PWs, (a) for different values of l_x, with the parameters $\kappa_p = 2$, $u = 0.1$, $q = 2$, $\delta = 1$, $p = 0.4$, $r = 3$, $\sigma = 0.05$, and $\Omega_{Bi} = 0.5$, (b) for different values of κ_p, with the parameters $u = 0.1$, $l_x = 0.6$, $q = 2$, $\delta = 1$, $p = 0.4$, $r = 3$, $\sigma = 0.05$ and $\Omega_{Bi} = 0.5$

10.57647/jtap.2026.2001.03

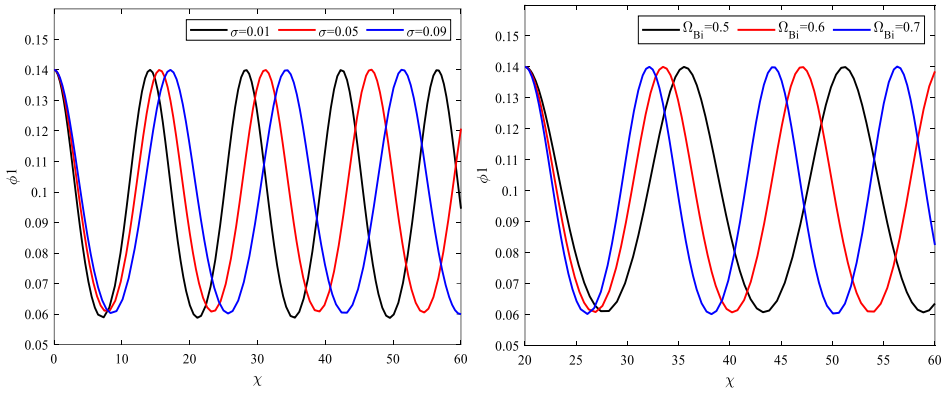

(a) (b)

Figure 9. The evolution of the PWs, (a) for different values of σ, with the parameters $\kappa_p = 2$, $u = 0.1$, $l_x = 0.6$, $q = 2$, $\delta = 1$, $p = 0.4$, $r = 3$, and $\Omega_{Bi} = 0.5$, (b) for different values of Ω_{Bi}, with the parameters $\kappa_p = 2$, $u = 0.1$, $q = 2$, $\delta = 1$, $p = 0.4$, $r = 3$, $\sigma = 0.05$, and $l_x = 0.6$

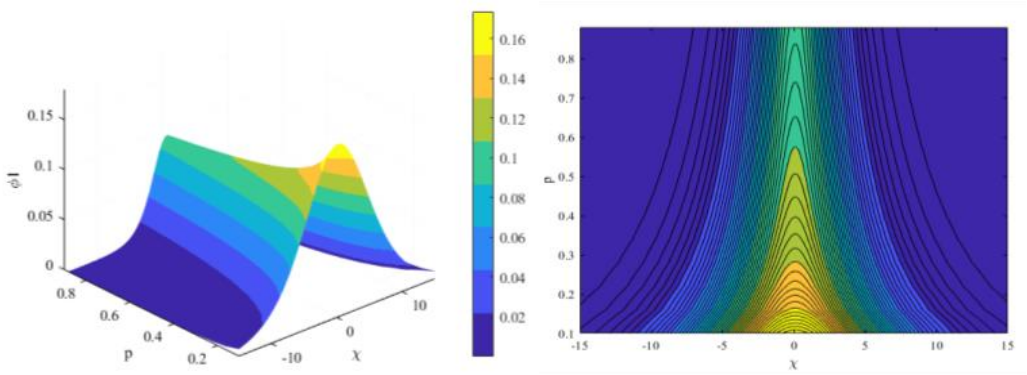

(a) (b)

Figure 10. Three-dimensional plot, (a) variation of ϕ^1 vs. p and χ, (b) contour plot of (a), with the parameters $\kappa_p = 2$, $u = 0.1$, $l_x = 0.8$, $r = 3$, $q = 2$, $\delta = 1$, $\sigma = 0.05$, and $\Omega_{Bi} = 0.5$

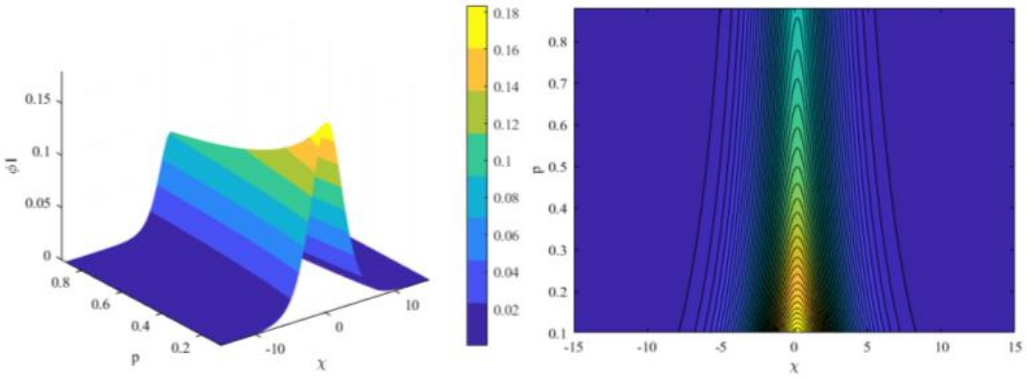

(a) (b)

Figure 11. Three-dimensional plot, (a) variation of ϕ^1 vs. p and χ, (b) contour plot of (a) , for the kappa limit case, with the parameters $\kappa_e = \kappa_p = 2$, $u = 0.1$, $l_x = 0.8$, $\delta = 1$, $\sigma = 0.05$, and $\Omega_{Bi} = 0.5$

It is clarified in Figure 9(b) that augmenting the background magnetic field effect Ω_{Bi} results in a decrease in the width of the IASWs without affecting the amplitudes. Figures 10-12 present three-dimensional graphical visualisations of IASWs and the respective contour plot diagrams. With the variation of the positron-to-electron density ratio (p), a three-dimensional SW profile is shown in Figure 10(a) as a function of space coordinate χ. It is observed that for the lowest value of p, the amplitude of the SW is raised, which agrees with the result obtained in Figure 5. The corresponding contour plot diagram is shown in Figure 10(b). The three-dimensional graphical representation of IASWs for the kappa limit is shown in Figure 11(a). The graphical representation clarifies that the amplitude of the SW goes spiky, and the profile makes itself in a compressed form as compared to that of Figure 10. The contour plot of Figure 11(a) is displayed in Figure 11(b).

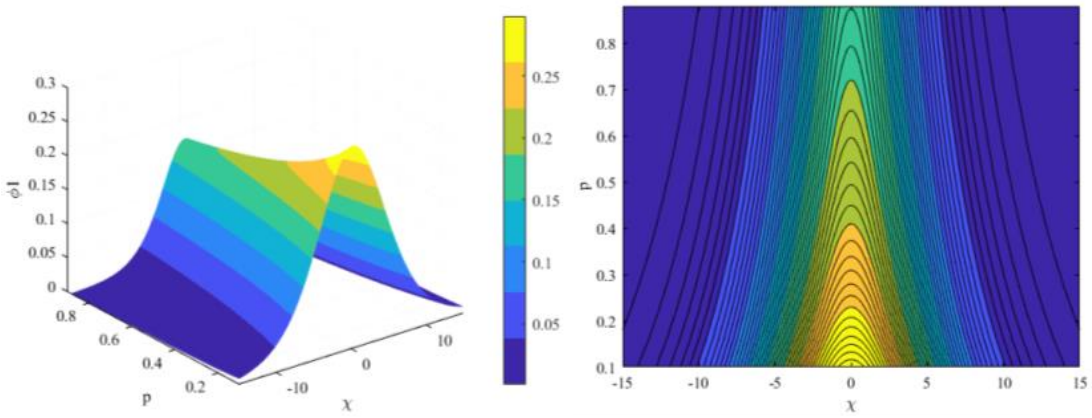

(a) (b)

Figure 12. Three-dimensional plot, (a) variation of ϕ^1 vs. p and χ, (b) contour plot of (a), for the Maxwellian limit case, with the parameters $\kappa_p = 2$, $r = 0$, $q \to \infty$, $u = 0.1$, $l_x = 0.8$, $\delta = 1$, $\sigma = 0.05$, and $\Omega_{Bi} = 0.5$

For the Maxwellian limiting case, the three-dimensional SW profile and the corresponding contour plot are displayed in Figures 12(a) and (b). The larger amplitude is seen in this particular condition as a comparison to that of earlier cases of (r, q)-distribution and κ -distribution limit.

5. Conclusions

This paper investigates the basic characteristics of ion-acoustic solitary and PWs formation in a superthermal magnetised plasma system containing electron and positron particles. Using the planar dynamical system corresponding to the ZK equation, the qualitative dynamics of the system are analysed. The numerical analysis shows that all the physical parameters significantly influence the formation of nonlinear waves. The important findings of these wave structures can be summarised as follows.

i. It can be analysed from the graphs in Figure 3(b) that the amplitude of the IASWs enhances as the value of wave velocity increases.

ii. The SW profile changing with the spectral index r, shown in Figure 4(b), reveals that the SW amplitude is diminished as it increases with the value of r.

iii. As evidenced in Figure 5(b), the positron-to-electron density ratio p has negative impacts on the amplitude and width of the SW.

iv. The graphical illustrations of nonlinear PWs in Figure 8(b) show that increasing the value of κ_p positively impacts both the amplitude and width of the PWs.

v. As evidenced in Figure 9(b), the background magnetic field effect does not change the amplitude but consistently decreases the width of the periodic waves.

vi. The three-dimensional graphical representations of IASWs in Figures 10(a), 11(a), and 12(a) show that in the case of the Maxwellian limit, the amplitude of the SW becomes larger in comparison to that of the kappa and (r, q)-distribution cases.

Declarations

Sources of Funds: No fund or grant was received for conducting this study.

Authors Contribution
The first author is the proposer and solver of the problem. The second author prepares the manuscript, and he connects different ideas about the results of the paper.

Availability of data and materials
No datasets were generated or analysed during the current study.

Conflict of interests
The authors declare that they have no conflicts of interest.

References

[1] F. Verheest; Waves and instabilities in dusty space plasmas. Space Sci Rev 77, 267-302 (1996). https://doi.org/10.1007/BF00226225

[2] P. K. Shukla; Nonlinear waves and structures in dusty plasmas. Phys. Plasmas 10, 1619-1627 (2003). https://doi.org/10.1063/1.1557071

[3] A. P. Misra, C. Bhowmik; Nonplanar ion-acoustic waves in a quantum plasma. Physics Letters A 369, 90-97 (2007). https://doi.org/10.1016/j.physleta.2007.04.066

[4] B. Tian, Yi-Tian Gao; Symbolic computation on cylindrical-modified dust-ion-acoustic nebulons in dusty plasmas. Physics Letters A 362, 283-288 (2007). https://doi.org/10.1016/j.physleta.2006.10.094

[5] N. Batool, I. Naeem, A. M. Mirza, W. Masood; Ion-acoustic vortex formation in a non-uniform two-electron-

temperature magnetoplasma with sheared ion flow. J. Plasma Physics 78, 65-69 (2012). https://doi.org/10.1017/S0022377811000390

[6] K. H. Shah, M. N. S. Qureshi, W. Masood, H. A. Shah; An alternative explanation for the density depletions observed by Freja and Viking satellites. AIP Advances 8, 085010 (2018). https://doi.org/10.1063/1.5040944

[7] H. Ikezi, R. Taylor, D. Baker; Formation and interaction of ion-acoustic solitons. Phys. Rev. Lett. 25, 11 (1970). https://doi.org/10.1103/PhysRevLett.25.11

[8] J. Zak; Finite translations in solid-state physics. Physical review letters 19, 1385-1387 (1967). https://doi.org/10.1103/PhysRevLett.19.1385

[9] C. Rebbi; Solitons. Scientific American 240, 92-117 (1979). https://www.jstor.org/stable/24965126

[10] M. G. Kivelson, J. A. Slavin, D. J. Southwood; Solitons in a Reaction-Diffusion System. Science 205, 493-495 (1979). https://doi.org/10.1126/science.205.4405.493

[11] T. Maxworthy, L. G. Redekopp; A Solitary Wave Theory of the Great Red Spot and Other Observed Features in the Jovian Atmosphere. Icarus 29, 261-271 (1976). https://doi.org/10.1016/0019-1035(76)90054-3

[12] H. Kikuchi; Shocks, solitons and the plasmapause. Journal of Atmospheric and Terrestrial Physics 38, 1055-1060 (1976). https://doi.org/10.1016/0021-9169(76)90033-7

[13] H. Washimi, T. Taniuti; Propagation Of Ion-Acoustic Solitary Waves Of Small Amplitude. Physical review letters 17, 996-998 (1966). https://doi.org/10.1103/PhysRevLett.17.996

[14] C.-R. Choi, C.-M. Ryu, K.-C. Rha, K.-W. Min, D.-Y. Lee; Ion-acoustic solitary waves in ion-beam plasma with Boltzmann electrons. Phys. Plasmas 19, 032105 (2012). https://doi.org/10.1063/1.3692049

[15] P. Goldreich, W. EL Julian; Pulsar Electrodynamics. The Astrophysical Journal 157, 869-880 (1969). https://doi.org/10.1086/150119

[16] S. K. El-Labany, W. M. Moslem, E. I. El-Awady; Nonlinear electrostatic excitations in a weakly relativistic electron-positron-ion rotating magnetoplasma. Physics of Plasmas 16, 102305 (2009). https://doi.org/10.1063/1.3243934

[17] M. C. Begelman, R. D. Blandford, M. J. Bees; Theory of extragalactic radio sources. Rev. Mod. Phys. 56, 255 (1984). https://doi.org/10.1103/RevModPhys.56.255

[18] Ph.-A. Bourdin; Plasma Beta Stratification in the Solar Atmosphere: A Possible Explanation for the Penumbra Formation. The Astrophysical Journal Letters 850, (2017). https://doi.org/10.3847/2041-8213/aa9988

[19] S. I. Popel, S. V. Vladimirov, P. K. Shukla; Ionacoustic solitons in electron-positron-ion plasmas. Physics of Plasmas 2, 716 (1995). https://doi.org/10.1063/1.871422

[20] Almas, Ata-ur-Rahman1, M. Khalid, S. M. Eldin; Oblique propagation of arbitrary amplitude ion acoustic solitary waves in anisotropic electron positron ion plasma. Front. Phys. 11, (2023). https://doi.org/10.3389/fphy.2023.1144175

[21] J. Kalita, R. Das, K. Hosseini, D. Baleanu, E. Hincal; Ion acoustic soliton with thermal ions and non-thermal electrons in a high-relativistic electron-positron-ion plasma. Partial Differential Equations in Applied Mathematics 8, 100579 (2023). https://doi.org/10.1016/j.padiff.2023.100579

[22] S. K. El-Labanya, W. M. Moslemb, E. I. El-Awadyb, P. K. Shuklad; Nonlinear dynamics associated with rotating magnetized electron-positron-ion plasmas. Physics Letters A 375, 159-164 (2010). https://doi.org/10.1016/j.physleta.2010.10.048

[23] K. Singh, N. Kaur, N. S. Saini; Head-on collision between two dust acoustic solitary waves and study of rogue waves in multicomponent dusty plasma. Phys. Plasmas 24, 063703 (2017). https://doi.org/10.1063/1.4984996

[24] J. Goswami, S. Chandra, B. Ghosh; Study of small amplitude ion-acoustic solitary wave structures and amplitude modulation in e-p-i plasma with streaming ions. Laser and Particle Beams 36, 136-143 (2018). https://doi.org/10.1017/S0263034618000058

[25] R. Sarma, A. P. Misra, N. C. Adhikary; Nonlinear ion–acoustic solitary waves in an electron-positron-ion plasma with relativistic positron beam. Chin. Phys. B 27, 105207 (2018). http://dx.doi.org/10.1088/1674-1056/27/10/105207

[26] P. Halder, K. N. Mukta, A. A. Mamun; Nonlinear Propagation of Dust-Ion-Acoustic Shock Waves in a Degenerate Multi-Species Plasma. Int J Cosmol Astron Astrophys 1, 81-87 (2019). https://doi.org/10.18689/ijcaa-1000119

[27] Shome, G. Banerjee; Bifurcation analysis of supernonlinear waves in an electron-positron-ion-dusty plasma having nonthermal distribution of electron and positron. Ricerche di Matematica 73, 725-739 (2024). https://doi.org/10.1007/s11587-021-00634-9

[28] S. K. El-Labany, W. M. Moslem, E. I. El-Awady; Nonlinear Langmuir structures: Soliton and shock in a rotating weakly relativistic electron-positron magnetoplasma with stationary positive ions. Physics of Plasmas 17, 062304 (2010). https://doi.org/10.1063/1.3439683

[29] P. Chatterjee, U. N. Ghosh; Head-on collision of ion acoustic solitary waves in electron-positron-ion plasma with superthermal electrons and positrons. Eur. Phys. J. D 64, 413-417 (2011). https://doi.org/10.1140/epjd/e2011-20155-7

[30] N. S. Saini, B. S. Chahal, A. S. Bains; Large amplitude dust ion-acoustic solitary waves in a plasma in the presence of positrons. Astrophys Space Sci 347, 129-138 (2013). 10.1007/s10509-013-1502-6

[31] K. Singh, A. Kakad, B. Kakad, N. S. Saini; Fluid simulation of ion acoustic solitary waves in electron-positron-ion plasma. Eur. Phys. J. Plus 136, 14 (2021). https://doi.org/10.1140/epjp/s13360-020-00941-4

[32] E. I. El-Awady, S. Hussain, N. Akhtar; Landau quantization effects on damping Kawahara solitons in electron-positron-ion plasma in rotating ionized medium. Commun. Theor. Phys. 76, 105502 (2024). 10.1088/1572-9494/ad5526

[33] W. Masood, M. N. S. Qureshi, P. H. Yoon, H. A. Shah; Nonlinear kinetic Alfvén waves with non-Maxwellian electron population in space plasmas. J. Geophys. Res. Space Physics 120, 101-112 (2015). https://doi.org/10.1002/2014JA020459

[34] T. Aziz, W. Masood, M. N. S. Qureshi, H. A. Shah, P. H. Yoon; Linear and nonlinear coupling of electromagnetic and electrostatic fluctuations with one dimensional trapping of electrons using product bi (r, q) distribution. Physics of Plasmas 23, 062307 (2016). https://doi.org/10.1063/1.4953428

[35] W. Masood, S. J. Schwartz, M. Maksimovic, A. N. Fazakerley; Electron velocity distribution and lion roars in the magnetosheath. Ann. Geophys., 24, 1725-1735 (2006). https://doi.org/10.5194/angeo-24-1725-2006

[36] J. Ozah and P. N. Deka; Dynamical behaviour of nonlinear structures in superthermal plasmas associated with external periodic force. Indian J Phys 97, 2197-2208 (2023). https://doi.org/10.1007/s12648-023-02603-4

[37] R. A. Cairns, A. A. Mamum, R. Bingham, R. Boström, R. O. Dendy, C. M. C. Nairn, P. K. Shukla; Electrostatic solitary structures in non-thermal plasma. Geophysical Research Letters 22, 2709-2712 (1995). https://doi.org/10.1029/95GL02781

[38] R. Boström; Observations of Weak Double Layers on Auroral Field Lines. IEEE Transactions On Plasma Science 20, 756-763 (1992). 10.1109/27.199524

[39] A. I. Eriksson, B. Holback, P. O. Dovner, Boström, G. Holmgren, M. Andre, L. Eliasson, P. M. Kintner; Freja observatons of correlated small-scale density depletions and enhanced lower hybrid waves. Geophysical Research Letters 21, 1843-1846 (1994). https://doi.org/10.1029/94GL00174

[40] M. N. S. Qureshi, J. K. Shi, S. Z. Ma; Landau damping in space plasmas with generalized (r, q) distribution function. Physics of Plasmas 12, 122902 (2005). https://doi.org/10.1063/1.2139504

[41] M. N. S. Qureshi, W. Nasir, W. Masood, P. H. Yoon, H. A. Shah, and S. J. Schwartz; Terrestrial lion roars and non-Maxwellian distribution. J. Geophys. Res. Space Physics, 119, 10,059-10,067 (2014). https://doi.org/10.1002/2014JA020476

[42] M. N. S. Qureshi, H. A. Shah, G. Murtaza, S. J. Schwartz, F. Mahmood; Parallel propagating electromagnetic modes with the generalized (r, q) distribution function. Physics Of Plasmas 11, 3819-3829 (2004). https://doi.org/10.1063/1.1688329

[43] S. Sehar, M. N. S. Qureshi, H. A. Shah; Electron acoustic instability in four component space plasmas with observed generalized (r, q)-distribution function. AIP Advances 9, 025315 (2019). https://doi.org/10.1063/1.5089197

[44] W. Albalawi, R. Jahangir, W. Masood, S. A. Alkhateeb, S. A. El-Tantawy; Electron-Acoustic (Un)Modulated Structures in a Plasma Having (r, q)-Distributed Electrons: Solitons, Super Rogue Waves, and Breathers. Symmetry 13, 2029 (2021). https://doi.org/10.3390/sym13112029

[45] Shumaila, R. Jahangir, F. Saba, A. W. Alrowaily, S. A. El-Tantawy; On the oblique electrostatic waves in a dusty plasma with non-Maxwellian electrons for Saturn's magnetosphere. Journal of Low Frequency Noise, Vibration and Active Control 43, 170-181 (2024). https://doi.org/10.1177/14613484231189625

[46] K. Habib, M. R. Hassan, S. Sultana, A. Mannan, A. A. Mamun; Dust-Acoustic Solitary Waves in an Electron-Depleted Nonthermal Magnetized Plasma. IEEE Transactions on Plasma Science 51, 3221-3233 (2023). 10.1109/TPS.2023.3308119

[47] A. Atteya, Reem Altuijri, Kottakkaran Sooppy Nisar, Abdel-Haleem Abdel-Aty, P. K. Karmakar, Eman Mohammed El-Bayoumi; Dynamics of Polarized Ion-Acoustic Waves in Magnetized Degenerate Multi Ions Plasma with Trapped Electrons: Nonlinear Periodic and Superperiodic Waves. Brazilian Journal of Physics 55, 133 (2025). https://doi.org/10.1007/s13538-025-01749-2

[48] M. M. Selim, A. El-Depsy, E. F. El-Shamy; Bifurcations of nonlinear ion-acoustic travelling waves in a multicomponent magnetoplasma with superthermal electrons. Astrophys Space Sci 360, 66 (2015). https://doi.org/10.1007/s10509-015-2574-2

[49] D. Kolay, D. Dutta, A. Saha; Modelling of nonlinear ion-acoustic wave structures due to Martian ionospheric loss. Astrophysics and Space Science 368, 4 (2023). https://doi.org/10.1007/s10509-022-04161-3

[50] D. Pradhan, D. Kolay, D. Dutta; Propagation Dynamics of Nonlinear Ion-Acoustic Waves in Multi-species Cometary Plasma with Kappa Distributed Electrons. Brazilian Journal of Physics 54, 166 (2024). https://doi.org/10.1007/s13538-024-01534-7

[51] S. Ali, W. Masood, H. Rizvi, R. Jahangir, Arshad M. Mirza; Contribution of the generalized (r, q) distributed electrons in the formation of nonlinear ion acoustic waves in upper ionospheric plasmas. AIP Advances 11, 125020 (2021). https://doi.org/10.1063/5.0075007

[52] A. Atteya, A. Saha, P. K. Karmakar, E. M. El-Bayoumi; Bifurcation analysis of electron-acoustic waves in electron beam-plasma with suprathermal electrons. Waves in Random and Complex Media, 1-17, (2024). https://doi.org/10.1080/17455030.2024.2358113

[53] S. Y. El-Monier, A. Atteya; Ion-acoustic waves dynamics in magnetized cometary plasma: nonlinear periodic and super-periodic waves with ion nonextensivity. Sci Rep 15, 7524 (2025). https://doi.org/10.1038/s41598-025-89765-9

[54] S. Khalid, M. N. S. Qureshi, W. Masood; Compressive and rarefactive solitary structures of coupled kinetic Alfven-acoustic waves in non-Maxwellian space plasmas. Phys. Plasmas 26, 092114 (2019). https://doi.org/10.1063/1.5115478

[55] S. Kouser, M. N. S. Qureshi, K. H. Shah, H. A. Shah; Ion-acoustic solitary waves in e-p-i plasmas with (r, q)-distributed electrons and kappa-distributed positrons. Contrib. Plasma Phys. 60, (2020). https://doi.org/10.1002/ctpp.202000058

[56] U. N. Ghosh, A. Abdikian, P. Chatterjee; Study of Multi-solitons, Breather Soliton Structures with (r, q) Distributed Ions and Electrons. Brazilian Journal of Physics 54, 218 (2024). https://doi.org/10.1007/s13538-024-01599-4

[57] R. Acharya, P. K. Prasad, A. Saha, A. Abdikian; Dust-Ion-Acoustic Jacobi Cnoidal, Dnoidal and Snoidal Wave Phenomena in a Magnetized Dusty Plasma with (r, q) Distributed Electrons. Brazilian Journal of Physics 54, 30 (2024). https://doi.org/10.1007/s13538-023-01378-7

[58] EI El-Awady, A. Abdikian, A. Saha; Nonlinear structure and growth rate of solitary waves for extended Zakharov-Kuznetsov equation in plasma having (r, q) distribution electrons. Phys. Scr. 99, 025605 (2024). https://doi.org/10.1088/1402-4896/ad1965

[59] J. Ozah, P. N. Deka; On the Bifurcation of Dust Ion-Acoustic Nonlinear Waves in a Magnetised Plasma with Energetic Electrons and Positrons. Brazilian Journal of Physics 54, 13 (2024). https://doi.org/10.1007/s13538-023-01381-y

[60] S. K. El-Labany, W. M. Moslem, F. M. Safy; Effects of two-temperature ions, magnetic field, and higher-order nonlinearity on the existence and stability of dust-acoustic solitary waves in Saturn's F ring. Phys. Plasmas 13, 082903 (2006). https://doi.org/10.1063/1.2336183

[61] A. Abdikian, S. Sultana; Dust-acoustic solitary and cnoidal waves in a dense magnetized dusty plasma with temperature degenerate trapped electrons and nonthermal ions. Phys. Scr. 96, 095602 (2021). 10.1088/1402-4896/ac04db

[62] A. Abdikian, J. Tamang, A. Saha; Supernonlinear wave and multistability in magneto-rotating plasma with (r, q) distributed electrons. Phys. Scr. 96, 095605 (2021). 10.1088/1402-4896/ac07b7

[63] A. Abdikian, J. Tamang, A. Saha; Investigation of supernonlinear and nonlinear ion-acoustic waves in a magnetized electron-ion plasma with generalized (r, q) distributed electrons. Waves in random and complex media. 34, 2615-2636 (2024). https://doi.org/10.1080/17455030.2021.1965242

[64] M. Khalid, A. Khan, M. Khan, F. Hadi. Ata-ur-Rahman; Dust Ion Acoustic Solitary Waves in Unmagnetized Plasma with Kaniadakis Distributed Electrons. Brazilian Journal of Physics. 51, 60-65 (2021).

https://doi.org/10.1007/s13538-020-00807-1

[65] S. Kouser, K. H. Shah, M. N. S. Qureshi, H. A. Shah; Nonlinear ion-acoustic waves in e-p-i plasmas with (*r*, *q*) distributed electrons and positrons. AIP Advances 10, 055123 (2020). https://doi.org/10.1063/5.0011128